A NEW APPROACH FOR CLOUD PARAMETER DETERMINATION IN THE 3I ALGORITHMS

C. J. Stubenrauch[+], A. Chedin[+], R. Armante[+], N. A. Scott[+], W. B. Rossow[#]

[+]Laboratoire de Météorologie Dynamique du CNRS, Ecole Polytechnique, Palaiseau, France

[#]NASA Goddard Space Flight Center, Institute for Space Studies, New York, USA

1. INTRODUCTION

The 3I (Improved Initialization Inversion) algorithms (Chedin and Scott 1985), as they have been developed in recent years, have provided in general reliable information from TOVS (TIROS-N Operational Vertical Sounder) observations (Smith at al. 1979) on cloud-top pressure and effective cloud amount, as has been shown (Stubenrauch et al. 1997a) in a comparison with time-space collocated clouds from the recently re-processed ISCCP (International Satellite Cloud Climatology Project) dataset (Rossow et al. 1996). Even low clouds were identified by the 3I cloud scheme (Stubenrauch et al. 1996), but systematic differences could be found in the Stratocumulus regions off the Western coasts, where 3I clouds were found mostly thinner and higher than the ISCCP clouds. In the case of low clouds, the method of mimimal dispersion of effective cloud amount used in the 3I cloud scheme as well as the well known CO_2-slicing method, due to a denominator getting near zero, are very sensitive to the chosen temperature profile and tend to determine the clouds as high thin rather than low opaque. For this reason, a χ^2 method, not including a denominator, has been developed, calculating effective cloud amount by using all CO_2-band channels, but with different weights depending on the effect of the brightness temperature uncertainty within an airmass on these channels at the various cloud levels.

2. ORIGINAL METHODS

In the IR (Infrared) Sounder community, mostly two approaches have been developed for the determination of cloud parameters:

1) One philosophy is to concentrate the determination of cloud-top pressure and effective cloud amount on high and midlevel clouds, because one estimates the instrument noise as being too high in the case of low clouds. In this case, Smith and Platt (1978), Susskind et al. (1987), Wylie and Menzel (1989) have used the CO_2-slicing method: The cloud-top pressure is determined by minimizing the function S in Eq. (1), slicing through the atmosphere with pairs of adjacent channels.

$$S(p_k) = \sum_{i,j=4,5...6,7} \left(\frac{I_m(\nu_i) - I_{clr}(\nu_i)}{I_m(\nu_j) - I_{clr}(\nu_j)} - \frac{I_{cld}^{i}(p_k,\nu_i) - I_{clr}(\nu_i)}{I_{cld}^{j}(p_k,\nu_j) - I_{clr}(\nu_j)} \right)^2 \qquad (1)$$

where ν_i and ν_j are two adjacent frequencies, I_m is the measured radiance, I_{clr} is the retrieved clear-sky radiance, I_{cld} is the calculated radiance emitted by a homogeneous opaque single cloud layer (ε=1), and θ is the viewing zenith angle. The effective cloud amount is then calculated by using Eq. (2). In order to get a complete information on all clouds, the amount of low clouds is determined using additional procedures.

2) The 3I cloud scheme (Stubenrauch et al. 1996, Wahiche et al. 1985) tries to extract cloud information at all heights by introducing the 'Coherence of effective cloud amount' method. Therefore, the CO_2-slicing method (Eq. 1) is applied only in a first step to eliminate cloud levels with $S(p_k)/S_{min} > 5$. For the remaining cloud levels and for each of the CO_2-band channels as well as for the 11μm IR window channel, one calculates the effective cloud amount in Eq. (2).

$$N\varepsilon(p_k,\nu_i) = \frac{I_m(\nu_i) - I_{clr}(\nu_i)}{I_{cld}(p_k,\nu_i) - I_{clr}(\nu_i)} \qquad (2)$$

with cloud levels k=1,30 and channels i = 4,...,8

Again, one assumes that all cloudy HIRS (High resolution Infrared Radiation Sound) pixels are covered by a homogeneous single cloud layer. After eliminating noisy channels i with $N\varepsilon(p_k,\nu_i)/\overline{N\varepsilon(p_k)} > 0.2$, one chooses the cloud-top pressure which leads to a minimum dispersion of Nε inside the CO_2-band. Local comparisons over the North Atlantic (Stubenrauch et al. 1996) with clouds identified from AVHRR (Advanced Very High Resolution Radiometer) measurements (Derrien et al. 1993) showed that even low clouds could be identified by the 3I cloud scheme.

Nethertheless, this method becomes unstable for low clouds, because the denominator in Eq. (2) gets towards zero. Figs. 1a and 1b show the difference I_{clr}-I_{cld} between clear and cloudy radiances as a function of cloud level for the five channels used in the cloud parameter extraction in two different geographical regions (a: Stratocumulus region off the West coast of Africa and b: Southern hemisphere ocean). One observes that the sounder weighting functions are involved in I_{clr}-I_{cld}, since for example I_{clr}-I_{cld} of channel 4, sounding the higher atmosphere, attains zero at higher cloud levels than I_{clr}-I_{cld} of channel 8, getting information down to the surface. Cloud levels 1 to 12 correspond to low clouds, and high clouds start from cloud level 20 upwards.

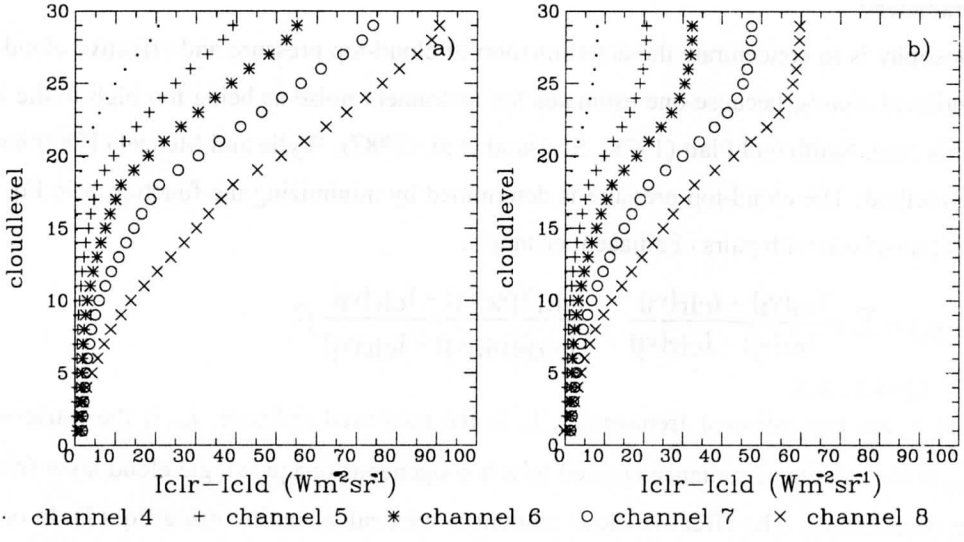

Figs. 1: Difference I_{clr}-I_{cld} between clear and cloudy radiances for the five HIRS channels used in cloud parameter determination at different cloud levels, for climatic conditions in January 1988, 7h30 am local time over a) the Stratocumulus region off the Westafrican coast and b) the Southern hemisphere ocean.

An error in the temperature profiles propagates into an error in I_{clr}-I_{cld}, which translates into an uncertainty in Nε. From Figs. 2a and 2b one observes that this uncertainty in Nε is highly asymmetric: it increases with increasing Nε, which means with decreasing cloud height.

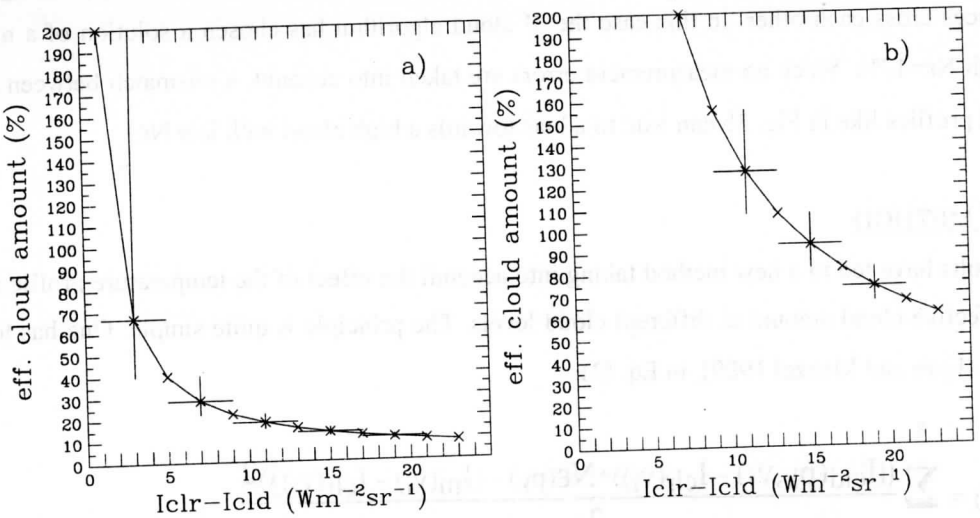

Figs. 2: Effective cloud amount Nε as a function of the difference I_{clr}-I_{cld} between clear and cloudy radiances, for climatic conditions in January 1988, 7h30 am local time for two examples of measured radiances: a) I_{clr}-I_m = 2 Wm^{-2}sr^{-1} and b) I_{clr}-I_m = 14 Wm^{-2}sr^{-1}. The error bars show the uncertainty in Nε due to an uncertainty of 2 Wm^{-2}sr^{-1} in I_{clr}-I_{cld}.

Figs. 3a and 3b give examples of 'IR radiance profiles' in the Stratocumulus region: IR radiances as seen by the five channels, with maximum contributions from the atmosphere around 400, 600, 800, 900 and 1000hPa. The profile with highest IR radiances is for a clear sky situation; then five different IR radiances are calculated for each cloud level, considering a single layer opaque cloud. The profiles are getting colder with increasing cloud level. One example cloud profile is shown for each case, together with the cloudy profile which was chosen by the 3I cloud algorithm. These are compared to the five IR radiances measured

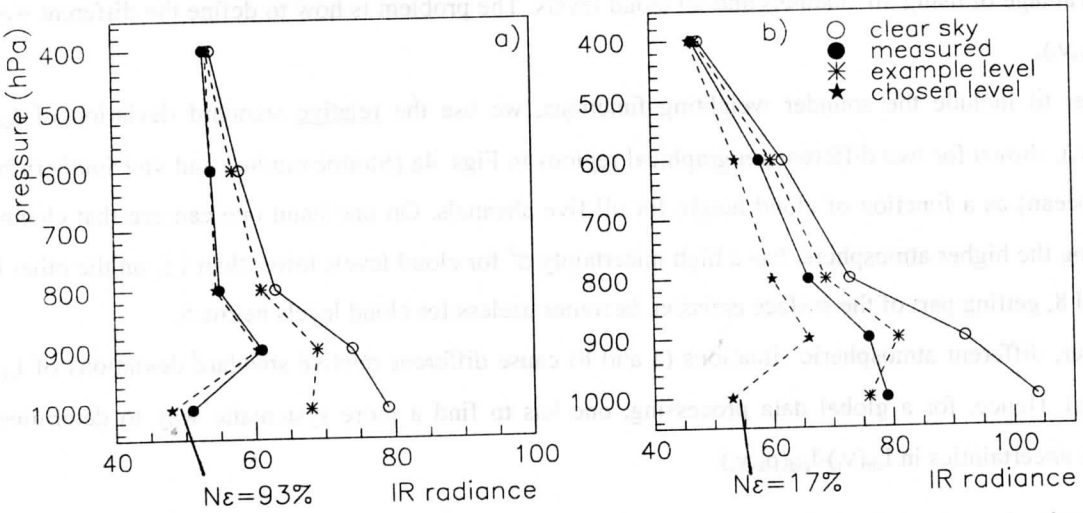

Figs. 3: a) and b) Two examples of 'IR radiance profiles' as seen by HIRS channels 4 to 8 are shown for clear sky, for a measured situation and for two different cloud levels. A mismatch in shape between the cloudy and measured profiles can lead to a higher cloud with smaller Nε.

by HIRS. Fig. 3a shows a situation in which the shape of the measured and the calculated 'IR radiance profile' agree quite well, leading to a solution with a nearly opaque cloud (Nε=93%). In comparison, Fig. 3b shows a case where the measured IR radiance profile and the one of the cloud level yielding the closest IR radiances cross each other. In this case the 3I cloud algorithm has chosen a solution of a much higher cloud with Nε=17%. Since no measurement errors are taken into account, a mismatch between cloudy and measured profiles like in Fig. 3b can lead to a bias towards a high cloud with low Nε.

3. χ^2 METHOD

These results have led to a new method taking into account the effect of the temperature profile uncertainty on the effective cloud amount at different cloud levels. The principle is quite simple: One has to minimize χ^2, like in (Eyre and Menzel 1989), in Eq. (3):

$$\chi^2(p_k) = \sum_{i=4}^{8} \frac{((I_{cld}(p_k,\nu_i) - I_{clr}(\nu_i))*N\varepsilon(p_k) - (I_m(\nu_i) - I_{clr}(\nu_i)))^2}{\sigma^2(p_k,\nu_i)} \qquad (3)$$

with weights $1/\sigma^2(p_k,\nu_i)$ depending on cloud level k and channel i with frequency ν_i, which should reflect the effect of the temperature profile uncertainty on the radiance difference $I_{clr}(\nu_i)$-$I_{cld}(p_k,\nu_i)$.

Minimizing χ^2 is equivalent to $d\chi^2/dN\varepsilon = 0$, from which one can extract Nε as:

$$N\varepsilon(p_k) = \frac{\Sigma((I_m(\nu_i) - I_{clr}(\nu_i)) (I_{cld}(p_k,\nu_i) - I_{clr}(\nu_i))/\sigma^2(p_k,\nu_i))}{\Sigma(I_{cld}(p_k,\nu_i) - I_{clr}(\nu_i))^2/\sigma^2(p_k,\nu_i)} \qquad (4)$$

One calculates Nε for all cloud levels k, and one chooses the solution with the minimal χ^2. This method has the advantage of using all channels and all cloud levels. The problem is how to define the different weights $1/\sigma^2(p_k,\nu_i)$.

In order to include the sounder weighting functions, we use the relative standard deviation of $I_{clr}(\nu_i)$-$I_{cld}(p_k,\nu_i)$, shown for two different geographical regions in Figs. 4a (Stratocumulus) and 4b (Southern hemispere ocean) as a function of cloud height for all five channels. On one hand one can see that channel 4, sounding the higher atmosphere, has a high uncertainty σ^2 for cloud levels lower than 15, on the other hand channel 8, getting part of the surface emisson, becomes useless for cloud levels below 5.

However, different atmospheric situations (a and b) cause different relative standard deviations of $I_{clr}(\nu_i)$-$I_{cld}(p_k,\nu_i)$. Hence, for a global data processing, one has to find a more systematic way to determine the relative uncertainties in $I_{clr}(\nu_i)$-$I_{cld}(p_k,\nu_i)$.

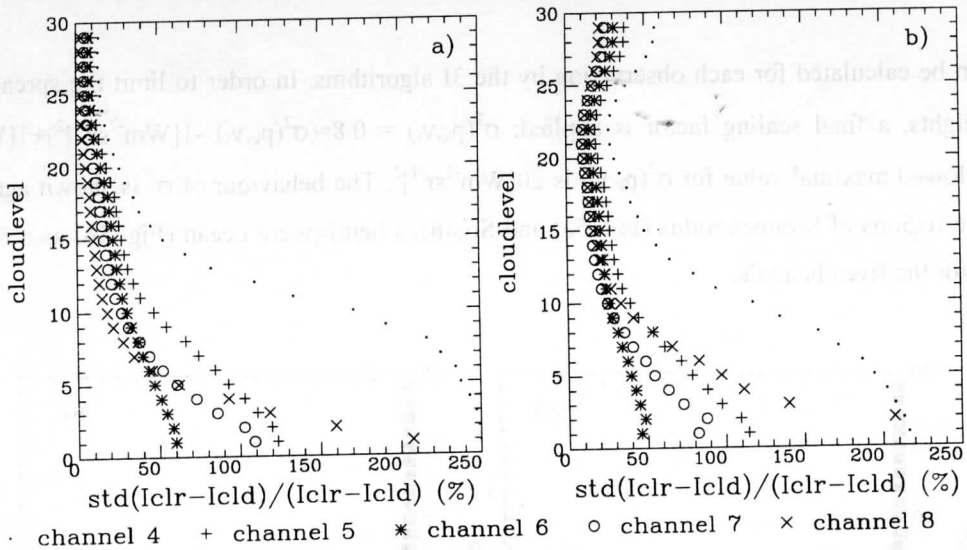

Fig. 4: Relative standard deviation of I_{clr}-I_{cld} as a function of cloud level for the five HIRS used in cloud parameter determination, for climatic conditions in January 1988, 7h30 am local time. a) over the Stratocumulus region off the Westafrican coast and b) over the Southern hemisphere ocean.

One way is to use the TIGR brightness temperature (T_b) standard deviations of the five channels within each of the five TIGR subsets of airmass types (Achard, 1991) as a measure of the temperature profile uncertainty. These vary from 3K to 10K, as one can see in Table 1.

channel / air	tropical	midlat.summer	midlat.winter	polar summer	polar winter
4	3.1K	5.0K	4.7K	3.8K	5.0K
5	2.8K	4.0K	3.6K	2.9K	3.2K
6	2.9K	3.8K	3.1K	2.9K	3.3K
7	3.4K	4.6K	3.7K	5.1K	5.5K
8	6.5K	8.7K	7.3K	9.6K	9.9K

Table 1: TIGR brightness temperature standard deviations (nadir viewing angle) within airmass type for the five HIRS channels used in the cloud parameter determination and for the five TIGR airmass type subsets.

The radiance I can be calculated from T_b as follows:

$$I = \frac{c_1}{\exp(c_2/T_b) - 1} \tag{5}$$

The uncertainty in T_b propagates into a radiance uncertainty dI:

$$dI = \frac{dI}{dT_b} dT_b = I \frac{c_2 \exp(c_2/T_b)}{T_b^2 \exp(c_2/T_b) - 1} dT_b \tag{6}$$

Finally, one can define $\sigma^2(p_k,\nu_i)$ as:

$$\sigma^2(p_k,\nu_i) = \frac{dI}{I_{cld}(p_k,\nu_i) - I_{clr}(\nu_i)} * 1[Wm^{-2}sr^{-1}]^2 \tag{7}$$

$\sigma^2(p_k,\nu_i)$ can be calculated for each observation by the 3I algorithms. In order to limit the spread between the 150 weights, a final scaling factor is applied: $\sigma^2(p_k,\nu_i) = 0.8*(\sigma^2(p_k,\nu_i) - 1[Wm^{-2}sr^{-1}]^2)+1[Wm^{-2}sr^{-1}]^2$. Also, the allowed maximal value for $\sigma^2(p_k,\nu_i)$ is $20[Wm^{-2}sr^{-1}]^2$. The behaviour of σ^2 is shown again for the two example regions of Stratocumulus (Fig. 5a) and Southern hemisphere ocean (Fig. 5b) as a function of cloud level for the five channels.

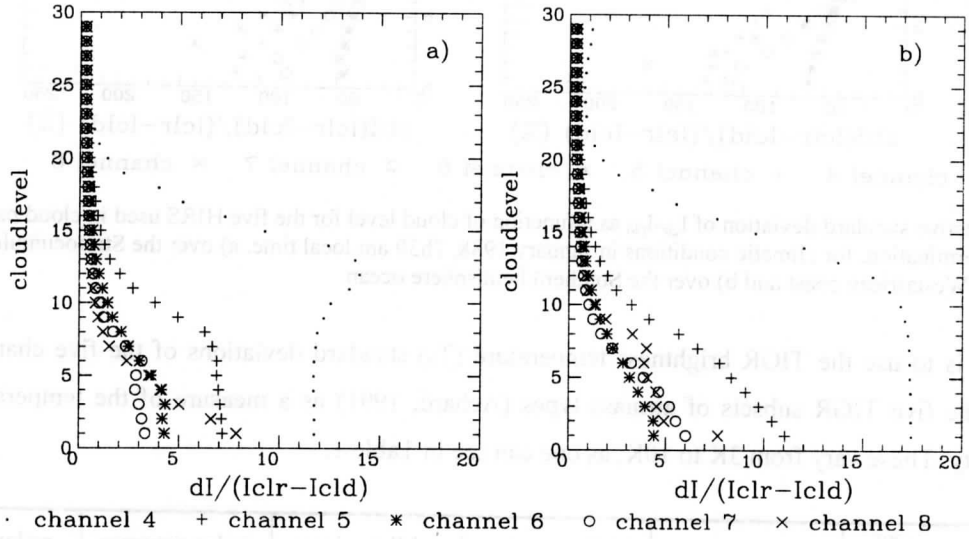

Fig. 5: $\sigma^2(p_k,\nu_i)$ as a function of cloud level for the five HIRS channels used in cloud parameter determination, for climatic conditions in January 1988, 7h30 am local time. a) over the Stratocumulus region off the Westafrican coast and b) over the Southern hemisphere ocean.

4. COMPARISON WITH ISCCP

For an evaluation of the 3I cloud parameters, we compare them with those obtained from AVHRR measurements processed by ISCCP (Rossow et al. 1996). One has to have in mind that both datasets are quite different: ISCCP cloud parameters come from one IR channel (11μm) and one VIS channel (0.6μm) (only during day) measurements with an initial spatial resolution of about 5km, sampled to 30km; 3I cloud parameters are determined from the average over all cloudy HIRS pixels (about 20km spatial resolution) within a 100km box, but using five IR CO_2-band channels, sounding into the atmosphere. Fig. 6 illustrates the different spatial behaviour of both datasets. Table 2 shows the matching of time-space collocated 3I-ISCCP cloud types in six different geographical regions: Northern hemisphere land (NL), North Atlantic (NA), Southern hemisphere midlatitude ocean (SH), Northern Stratocumulus (STN), Southern Stratocumulus (STS) and Tropical Warm Pool (WP). For this matching study, four cloud types have been defined: high opaque, cirrus, midlevel and lowlevel clouds. Agreement is achieved when the 3I cloud type is the same as the most frequent ISCCP cloud type inside the same 1° grid. More details about the comparison can be found in (Stubenrauch et al. 1997b).

region:	NL	NA	SH	STN	STS	WP
3I-ISCCP match	40.6%	46.2%	53.2%	49.5%	50.8%	47.5%
new3I-ISCCP match	47.4%	64.7%	64.1%	76.4%	72.8%	60.8%

Table 2: 1° time-space collocated 3I-ISCCP cloud type matching agreement in six different geographical regions, 3I cloud types determined by the original 3I cloud scheme and by the χ^2 method.

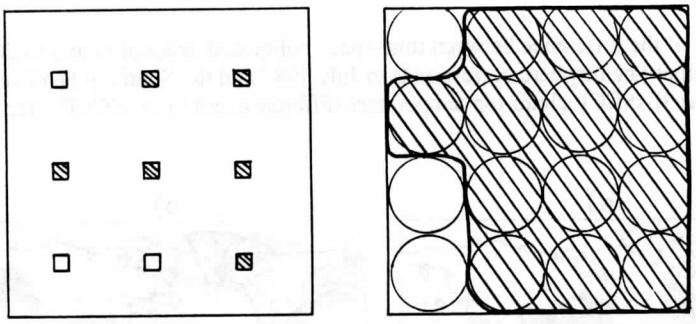

Fig. 6: Illustration of a 1°grid filled on one hand by 5km large ISCCP pixels (hatched if cloudy), sampled every 30km and on the other hand by 20km large HIRS pixels (hatched if cloudy).

Figs. 7 and 8 show geographical maps of the difference between time-space collocated 3I and ISCCP cloud parameters: a) cloud-top temperature and b) effective cloud amount. In the ISCCP dataset, the effective cloud amount has to be calculated from the optical thickness of cloudy pixels inside a 1° grid (see section 3.2 in Stubenrauch et al. 1997b). In Figs. 7, the 3I algorithm is the one described in (Stubenrauch et al. 1996), whereas Figs. 8 show the results of the new 3I cloud scheme using the χ^2 method. By looking at the cloud-top temperature difference in Fig. 7a, one observes for about half of the globe an agreement within 5K between ISCCP and 3I. Over land, 3I identifies warmer clouds than ISCCP, a mismatch due to the difficult distinction between partly cloudy low clouds and Cirrus. Another feature are lower cloud-top temperatures in the ITCZ (Intertropical Convergence Zone), mostly due to larger Cirrus regions determined by 3I. Considering the effective cloud amount difference in Fig. 7b, one observes a systematic underestimation by the original 3I cloud scheme in all Stratocumulus regions; in other regions with mostly low clouds the difference is less significant. Another problematic zone is the sea ice region off the coast of Antarctica, where probably ISCCP underestimates the cloud cover. The results in this zone did not change with the new χ^2 scheme, further studies with additional datasets are needed here. On the other hand, using the χ^2 scheme, the Nε structures in all Stratocumulus regions disappear, leading globally to a much better agreement between ISCCP and 3I. Also the cloud-top temperatures in Fig. 8a agree much better, leaving only some regions like the Sahara and some parts of the Northern hemisphere land with disagreement due to misidentification between Cirrus and partly cloudy low clouds.

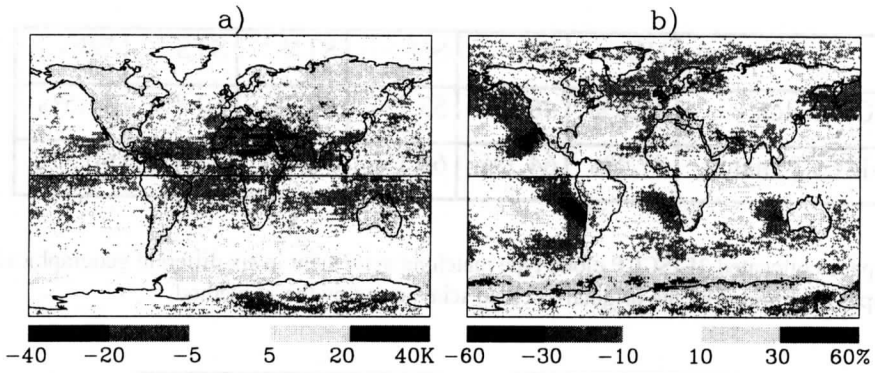

Figs. 7: Geographical maps of the difference between time-space collocated original 3I and ISCCP cloud parameters during day: The Northern hemisphere corresponds to July 1987 and the Southern hemisphere to January 1988, 7h30 am local time.a) 3I-ISCCP cloud-top temperature difference and b) 3I-ISCCP effective cloud amount difference.

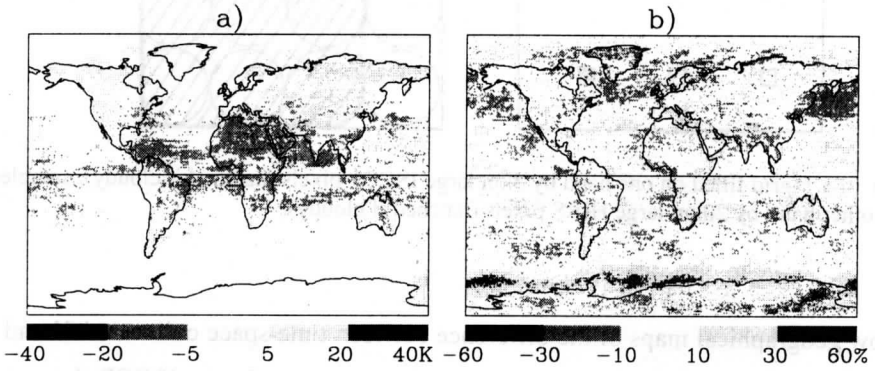

Figs. 8: Geographical maps of the difference between time-space collocated 3I (χ^2 mehod) and ISCCP cloud parameters during day: The Northern hemisphere corresponds to July 1987 and the Southern hemisphere to January 1988, 7h30 am local time.a) 3I-ISCCP cloud-top temperature difference and b) 3I-ISCCP effective cloud amount difference.

In July, the 3I temperature profiles are colder in the lower atmosphere and warmer in the upper atmosphere than the operational TOVS temperature profiles used in ISCCP. This effect is more strongly pronounced in the midlatitudes and tropics as one can see in Figs. 9a to 9c. The difference in temperature profiles explains that 3I sees low clouds lower and high clouds higher, leading to a wider spread of cloud-top pressure and to a bimodal structure in effective cloud amount weighted cloud-top pressure distributions, shown in Figs. 10a to 10d for four different geographical regions. The same bimodal structure has been observed by Susskind at al. (1997). ISCCP produces distributions with one broad maximum. The effective cloud amount weighted cloud-top temperature distributions in Figs. 11a to 11d agree already better. Differences in the midlatitudes can be explained by lower Nε from 3I at lower temperatures due to heterogeneous regions; and in the Tropical Warm Pool where one expects more than 30% lowlevel clouds underneath cirrus clouds (Jin and Rossow 1997) ISCCP misidentifies these as partly cloudy lowlevel clouds.

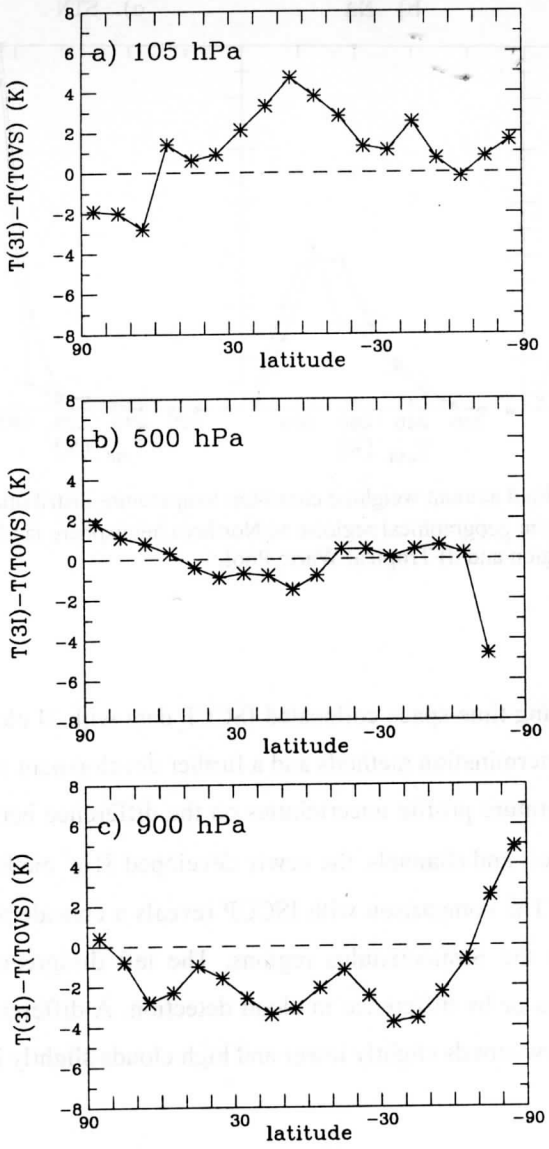

Figs. 9: Monthly mean temperature differences between 3I and the operational TOVS used in ISCCP a) around 105 hPa b) around 500 hPa and c) around 900 hPa for July 1987.

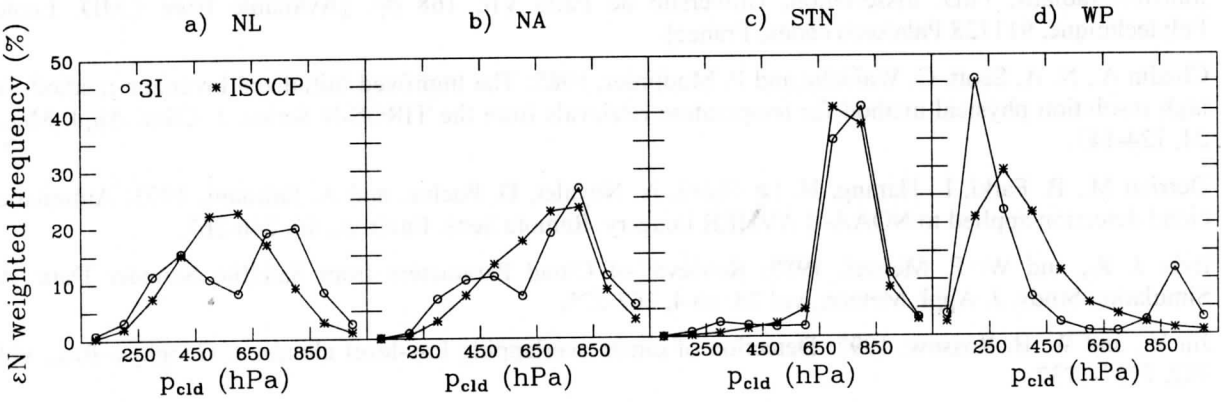

Figs. 10: Monthly mean effective cloud amount weighted cloud-top pressure distributions determined by 3I (O) and by ISCCP (*) in four different geographical regions: a) Northern hemisphere land, b) North Atlantic, c) Northern Stratocumulus region and d) Tropical Warm Pool.

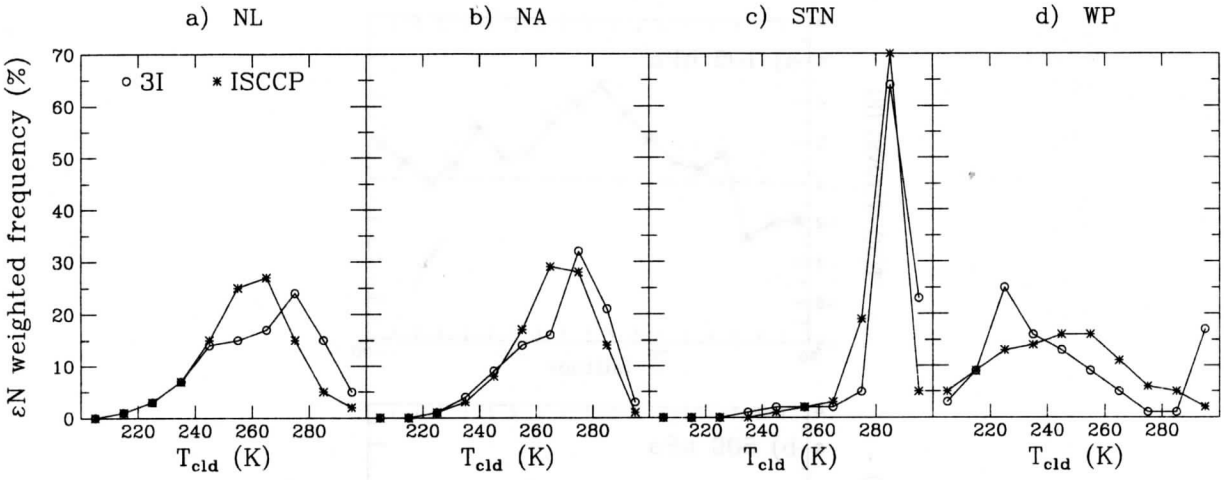

Figs. 11: Monthly mean effective cloud amount weighted cloud-top temperature distributions determined by 3I (O) and by ISCCP (*) in four different geographical regions: a) Northern hemisphere land, b) North Atlantic, c) Northern Stratocumulus region and d) Tropical Warm Pool.

5. CONCLUSIONS

The iterative process of comparing time-space collocated ISCCP data with 3I cloud parameters has led to a review of IR cloud parameter determination methods and a further development of these methods. By taking into account the effect of temperature profile uncertainties on the difference between clear sky and cloudy radiances for different cloud levels and channels, the newly developed 3I χ^2 method yields non-biased cloud parameters at all cloud heights. The comparison with ISCCP reveals a considerable improvement of the 3I cloud parameters, especially in the Stratocumulus regions. The left disagreements with ISCCP can be explained by grid heterogeneities or by difference in cloud detection. A difference in temperature profiles explains the fact that 3I places low clouds slightly lower and high clouds slightly higher than ISCCP.

6. REFERENCES

Achard V., 1991: Trois problèmes clés de l'analyse 3D de la structure thermodynamique de l'atmosphère pas satellite: Mesure du contenu en ozone; classification des masses d'air; modélisation 'hyper' rapide du transfert radiatif. PhD. dissertation, Université de Paris VII, 168 pp. [Available from LMD, Ecole Polytechnique, 911128 Palaiseau cedex, France]

Chedin A., N. A. Scott, C. Wahiche and P. Moulinier, 1985: The Improved Initialized Inversion method: A high resolution physical method for temperature retrievals from the TIROS-N Series. J. Clim. Appl. Met., 24, 124-143.

Derrien M., B. Farki, L. Harang, H. Le Gléau, A. Noyalet, D. Pochic, and A. Sairouni, 1993: Automatic cloud detection applied to NOAA-II AVHRR imagery. Remote Sens. Environ., 46, 246-267.

Eyre J. R., and W. P. Menzel, 1989: Retrieval of Cloud Parameters from Satellite Sounder Data: A Simulation Study, J. Appl. Meteor., vol 28, no 4, 267-275.

Jin Y., and W. B. Rossow, 1997: Detection of cirrus overlapping low-level clouds, J. Geophys. Res., vol 102, 1727-1737.

Menzel W. P., D. P. Wylie and K. I. Strabala, 1997: Seven Years of Global Cirrus Cloud Statistics using HIRS, subm. to J. Clim.

Rossow W. B., A. W. Walker, D. Beuschel and M. Roiter, 1996: International Satellite Cloud Climatology Project (ISCCP): Description of New Cloud Datasets. WMO/TD-No.737, World Climate Research Programme (icsu and WMO), Geneva, February 1996, 115pp.

Smith W. L., and C. M. R. Platt, 1978: Intercomparison of radiosonde, ground based laser and satellite deduced cloud heights. J. Appl. Met., 17, 1796-1802.

Smith W. L., H. M. Woolf, M. C. Hayden, D. Q. Wark, and L. M. McMillin, 1979: The TIROS-N Operational Vertical Sounder. Bull. Am. Met. Soc., 60, 1177-1187.

Stubenrauch C. J., N. A. Scott and A. Chedin, 1996: Cloud Field Identification for Earth Radiation Budget Studies: I) Cloud Field Classification using HIRS/MSU Sounder Measurements, J. Appl. Met., Vol 35, 416-427.

Stubenrauch C. J., W. B. Rossow, F. Chéruy, N. A. Scott, and A. Chedin, 1997a: Combining 3I Cloud Parameters and ISCCP for better understanding of Cloud Radiative Effects, IRC Symposium Proceedings, Fairbanks, Alaska, 19-24 August 1996, 4 pp.

Stubenrauch C. J., W. B. Rossow, F. Chéruy, N. A. Scott, and A. Chedin, 1997b: Combining 3I Cloud Parameters and ISCCP for better understanding of Cloud Radiative Effects, International TOVS meeting Proceedings, Igls, Austria, 19-24 February 1997, 12 pp.

Susskind J., D. Reuter, and M. T. Chahine, 1987: Cloud fields retrieved from analysis of HIRS2/MSU sounding data. J. Geophys. Res., 92 (D4), 4035-4050.

Susskind J., P. Piraino, L. Rokke, L. Iredell and A. Mehta, 1997: Characteristics of the TOVS Pathfinder Path A Data Set, subm. to Bull. Am. Met. Soc.

Wahiche, C. N., N. A. Scott and A. Chedin, 1986: Cloud detection and cloud parameter retrieval fromthe satellites of the TIROS-N series, Ann. Geophys., 4B, 2, 207-222.

Wylie D. P., and W. P. Menzel, 1989: Two years of cloud cover statistics using VAS, J. Climate, 2, 380-392.

TECHNICAL PROCEEDINGS OF

THE NINTH INTERNATIONAL TOVS STUDY CONFERENCE

Igls, Austria

20-26 February 1997

Edited by

J R Eyre

Meteorological Office, Bracknell, U.K.

Published by

European Centre for Medium-range Weather Forecasts
Shinfield Park, Reading, RG2 9AX, U.K.

May 1997